

Valorization of edible industrial and agricultural food byproducts for rheological properties and 3D printability in food inks

Ling Xin Yong ^{a,c}, Xin Ying Fiona Lim ^a, Say Chye Joachim Loo ^{a,b,c,*}

^a School of Materials Science and Engineering, Nanyang Technological University, 50 Nanyang Avenue 639798, Singapore

^b Lee Kong Chian School of Medicine, Nanyang Technological University, 59 Nanyang Drive 636921, Singapore

^c Singapore Centre for Environmental Life Sciences Engineering, Nanyang Technological University, 60 Nanyang Drive 637551, Singapore

ARTICLE INFO

Keywords:

Additive manufacturing

Sequential study

Food waste valorization, Rheological properties, Food bioprinting

ABSTRACT

Food waste generated from food manufacturing byproducts and agricultural surplus is a pressing global concern, leading to the loss of valuable nutrients and environmental challenges. This study explores the use of different hydrogels as a sustainable carrier for incorporating this edible food by product commonly regarded as food waste into 3D food printing (3DFP) inks, aiming to reduce nutrient wastage while promoting sustainable practices in food manufacturing. Four types of food waste – okara, sesame cake (SC), brewer's spent grain (BSG), and butterhead lettuce, were investigated for their particle morphology, water hydration capacity (WHC), and tap density. These properties are crucial as they determine the rheology and printability of the 3DFP ink. Rheological evaluations identified 5 % w/v thermoplastic (TPS) gel as the optimal base material, offering favorable gel-like properties, good structural integrity and flowability during printing during extrusion 3DFP. Among the tested inks, 20 % w/v BSG and lettuce exhibited the most consistent and stable printing performance, with mean viscosities of 4016.7 mPa·s and 6330.4 mPa·s at a shear rate of 100 1/s. Okara, which has the highest WHC led to ink drying and instability, even at reduced concentrations, while SC's high density caused nozzle clogging due to particle agglomeration and separation from gel phase. This study demonstrates the potential of valorizing food waste by leveraging its fiber and protein content to create functional 3DFP inks. By transforming zero-cost food waste into printable food inks, this research offers innovative solutions for sustainable food preparation, reducing landfill waste, and advancing environmentally responsible manufacturing methodologies.

Introduction

Food goes through a lengthy supply chain process of farming, manufacturing, and distribution before it arrives at our kitchen table. (Malik et al., 2018; Zhong et al., 2017) During these processes, substantial amounts of byproducts and surplus are often disposed of as industrial or agricultural “food waste”. (Handayati and Widyanata, 2024; Chauhan et al., 2021) In Singapore alone, 40 % of the 744,000 tons of food waste in 2019 were generated by commercial and industrial entities. (National Environment Agency NEA Singapore, 2021) However, most of these homogeneous “food wastes” are also edible food products themselves that possess nutritional profiles far beyond general comprehension. (Oyedeleji and Wu, 2023; Asghar et al., 2023; Wan et al., 2023) With population growth and rising food demand, other plausible ideas to address this demand are to utilize edible “food waste” by valorizing them into alternative food options. Valorization of industrial

food waste can: (i) promote food security by providing an additional food source, (ii) generate more food sources without the need to scale up current production, and (iii) lead to fewer byproducts and food surplus that end up in landfill. (National Environment Agency; Agri-Food & Veterinary Authority of Singapore, 2017)

Such edible food waste, rich in nutrients and derived from commonly consumed ingredients, presents significant potential for reuse. For example, sesame cake (SC), a byproduct of sesame oil, contains defatted sesame seeds with high protein content. (Wan et al., 2023) Okara, which is the residue from soymilk extraction, and brewer's spent grain (BSG), a brewing byproduct, are both high in fiber and protein. (Asghar et al., 2023; Lynch et al., 2016) These food wastes are not only homogeneous but also readily available in large quantities across many countries, particularly in Asia where soymilk consumption and sesame oil usage are high. They are often widely recognized for their high potential in valorization into functional and sustainable food applications. (Oyedeleji

* Corresponding author.

E-mail address: joachimloo@ntu.edu.sg (S.C.J. Loo).

and Wu, 2023; Asghar et al., 2023; Wan et al., 2023; Lynch et al., 2016; Fu et al., 2017; Lee et al., 2021; Zeko-Pivač et al., 2022; Amoriello et al., 2020; Farcas et al., 2021) One common upcycling approach involves transforming food byproducts into new products, such as making bread from BSG or extracting functional ingredients from fruit and vegetable peels. (Amoriello et al., 2020; Sagar et al., 2018; Lau et al., 2021) Okara has also gathered attention for its versatility, being used as a fermented ingredient to enhance the sensory properties of plant-based meat, or in its unfermented form as a prebiotic soy flour alternative. (Asghar et al., 2023; Razavizadeh et al., 2021)

An innovative approach for utilizing edible food waste is 3D food printing (3DFP). Using a layer-by-layer additive manufacturing technique, 3DFP offers precise control over composition, texture, and aesthetics. It streamlines food preparation, facilitates nutrient customization by incorporating supplements like probiotics directly into inks, and enhances visual appeal. (Liu et al., 2020; Voon et al., 2019) A recent review by Yoha and Moses highlighted studies on valorizing food waste through 3DFP, (Yoha and Moses, 2023) such as potato byproducts in yam snacks, cod fish byproducts for surimi, and soybean byproducts in cookies, demonstrating the potential of sustainable ingredients (Feng et al., 2020; Gudjónsdóttir et al., 2019; Lee et al., 2021; Zhang et al., 2022).

3DFP is particularly appealing for applications requiring dietary customization. (Escalante-Aburto et al., 2021) For dysphagic patients, enhancing the visual appeal and palatability of softer-textured foods improves their appetite and acceptance. (Zhang et al., 2024; Mirazimi et al., 2022; Pant et al., 2021) Furthermore, 3DFP can be useful when nutrition customization is required for people with conditions including diabetes, kidney disease, or specific allergies. While various 3D printing processes are available, extrusion-based 3DFP is preferred for its scalability and versatility. (Waseem et al., 2024) In extrusion 3DFP, a hydrogel carrier such as xanthan gum or gelatine is often required to maintain layer integrity. (Sharma et al., 2024; Baiano, 2022) Key considerations for 3DFP inks include the use of food safe non-toxic ingredients, ideally those classified as Generally Recognized as Safe (GRAS), along with achieving optimal rheological properties to ensure consistent extrusion, layer stability, and shelf life. (Mirazimi et al., 2022)

Despite the potential of 3DFP for food waste valorization, previous studies have explored only a limited number of food waste types and have largely overlooked the influence of particle characteristics on printability. (Yoha and Moses, 2023; Hooi Chuan Wong et al., 2022) Rheological parameters such as viscosity, yield stress, and viscoelasticity are critical for the 3DFP process, as they directly influence flow through the nozzle, shape retention after deposition, and the ability to support multiple layers. (Voon et al., 2019; Tejada-Ortigoza and Cuan-Urquiza, 2022) In the context of food waste valorization, understanding and tuning these properties is essential for ensuring printability and reproducibility. This provides a more practical foundation for developing sustainable, printable food inks from real-world waste sources.

While previous studies have focused on limited food materials or model hydrogels, our study extends this knowledge by examining diverse food-waste streams with varying compositions and assessing their rheological behavior in relation to print performance. To address these gaps, this study investigates the rheological properties of three hydrogels - alginate, KC, and thermoplastic starch (TPS), evaluating their compatibility with diverse food waste types, including lettuce, okara, SC, and BSG. By analyzing the interactions between hydrogel matrices and food waste particles, this study aims to develop optimized and stable 3DFP inks, thereby advancing sustainable food manufacturing and contributing to waste reduction.

Materials & methods

Materials

The food wastes were provided by industries: brewer's spent grain

(BSG) was from Par International Pte. Ltd., sesame cake (SC) was from Oh Chin Hing Sesame Oil Factory, and okara was from Super Bean International Pte. Ltd. TPS was prepared using tapioca starch (Flying Man brand by Ng Nam Bee Marketing Pte. Ltd.), purchased from NTUC supermarket in Singapore. Reagent-grade glycerol, sodium alginate and kappa carrageenan (KC) were purchased from Sigma Aldrich Pte. Ltd.

Methods

Pre-processing of food waste

The lettuce had its roots removed, and the lettuce leaves were rinsed with tap water and dried before it was left in the -20°C freezer overnight. Upon receiving the okara, BSG and SC were immediately stored in a -20°C freezer. Following that, all the food wastes were placed in a freeze dryer (Labconco FreeZone2.5) for at least 48 - 120 h to remove all moisture in the sample. Freeze-dried lettuce and SC were broken down with a high speed kitchen blender (Philips Blender HR2056/21 – Dry Mill). Okara and BSG came in ground form and did not require further blending. All food wastes were then sieved through a 50-mesh (508 μm) prior to blending with hydrogel, forming 3DFP inks. The process is illustrated as per Fig. 1.

Preparation of hydrogel

A stock solution of the hydrogel – 1 % w/v alginate, 2 % w/v alginate, 3 % w/v alginate, and 1 % w/v KC was prepared individually with deionized (DI) water. The selection of hydrogel percentages was guided by commonly explored concentrations for each type of hydrogel. Both KC and alginate hydrogel are typically explored in the range of 1 – 3 % w/v. However, KC of 2 and 3 % w/v were solid-state gel at room temperature, hence the study only proceeded at a 1 % w/v KC. (Tomić et al., 2023; Al-Baari et al., 2018; Wang et al., 2023) Fig. 1 shows the process of weighing and mixing. After the solid component was added into DI water, the mixture was allowed to mix overnight with a magnetic stirrer hotplate (heidolph) at 500 rpm and at room temperature. 2 % w/v and 3 % w/v alginate required additional heating at 45°C for 15 min. A stock solution was considered ready when all powder had fully dissolved.

Preparation of TPS gel

5 % w/v of tapioca starch powder was manually mixed with glycerol (2.5 % v/v) as a plasticizer in DI water as per Fig. 1. For TPS, 5 % w/v of starch was used as this was based on the lowest percentage to achieve gelatinized starch. (Chakraborty et al., 2022) The mixture of tapioca starch, glycerol, and DI water was stored in ambient conditions for 24 h in a closed glass container/ beaker before being heated in a water bath setup with continuous magnetic stirring the subsequent day. The water bath was heated up to 65°C on a magnetic stirrer hotplate, and it took about 30 min to 40 min to obtain TPS, depending on the quantity prepared.

Preparation of 3D food printing (3DFP) inks

The hydrogel was manually mixed with food waste particles in different percentages using a spatula and a beaker until there was no visible food waste particle, Fig. 1. Formulation details of the 3DFP inks prepared are shown as per Table 1.

Tap density

The tap density of the food waste particles was determined using a standardized procedure to ensure consistent results across all samples. A clean and dry 4 mL glass vial was used for each measurement. First, the empty vial was weighed using an analytical balance to record its tare weight. The food waste was then filled into the vial manually using a spatula. When the food waste reached the 25 % mark based on the volume of the vial, the vial was manually tapped ten times. Additional food waste was added incrementally until the vial reached 50 %, 75 %, and finally 100 % of its capacity, with each step followed by ten manual

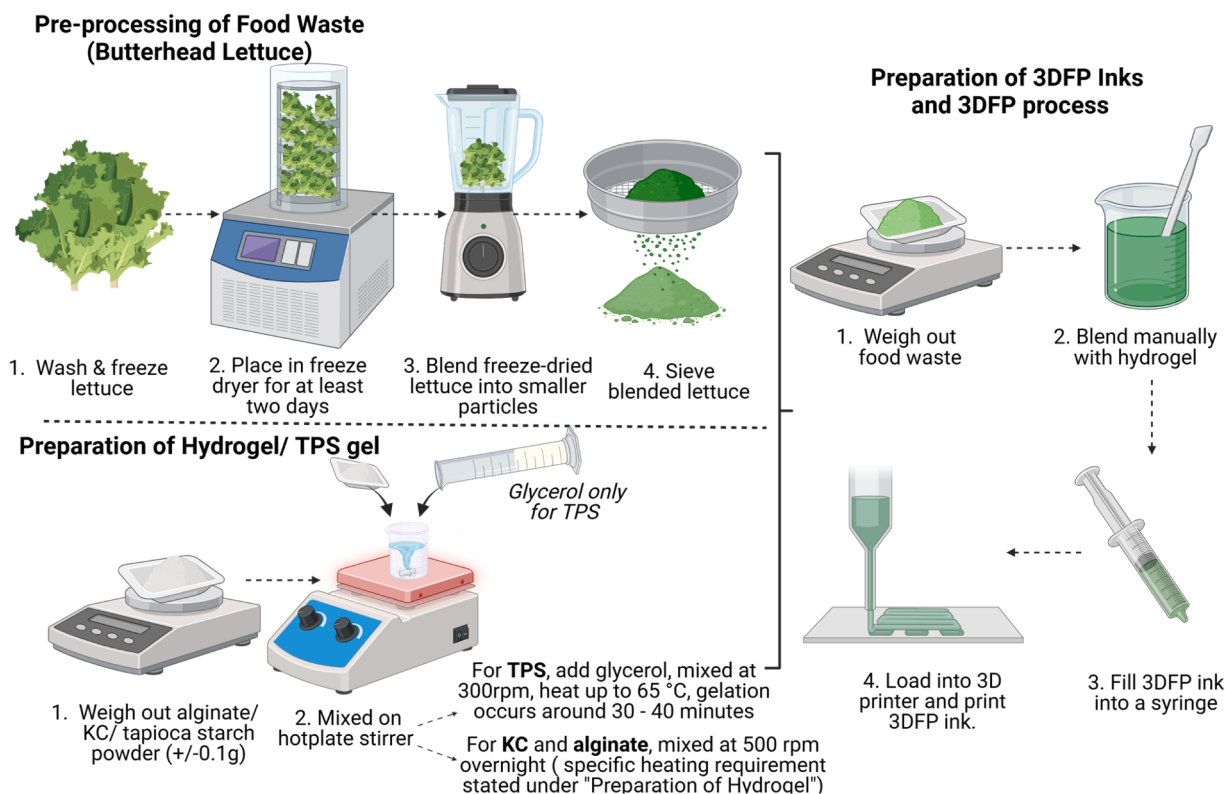


Fig. 1. Schematic flow chart of the pre-processing of butterhead lettuce, preparation of hydrogel/ TPS gel, preparation of 3DFP inks and 3DFP process. Created in BioRender. Yong, L. (2025) <https://BioRender.com/y30m689>.

Table 1
The percentage ratio of all the 3DFP inks prepared in this study.

Raw Materials	5 % w/v Lettuce 1 % w/v KC	5 % w/v Lettuce 5 % w/v TPS	10 % w/v Lettuce	20 % w/v Lettuce	30 % w/v Lettuce	20 % w/v BSG	30 % w/v BSG	20 % w/v SC	30 % w/v SC	10 % w/v Okara
Hydrogel	95	95	90	80	70	80	70	80	70	90
Lettuce	5	5	10	20	30	-	-	-	-	-
BSG	-	-	-	-	-	20	30	-	-	-
SC	-	-	-	-	-	-	-	20	30	-
Okara	-	-	-	-	-	-	-	-	-	10

taps to ensure uniform packing. Once the vial was filled to the 100 % mark and tapped ten times, food waste was added incrementally until the vial reached the 4 mL neck mark, and the volume stabilized with ten additional taps. The filled vial was weighed to obtain the mass of the food waste, and the tap density was calculated as the ratio of the mass of the food waste to the volume of the vial. Care was taken to perform the tapping and filling steps consistently to minimize variability.

Water hydration capacity (WHC) of food waste particles

The water hydration capacity (WHC) evaluation of the food waste particles was modified with reference to protocol from Kim et al. (Kim et al., 2018). To begin, 0.10 g (m_i) of food waste was weighed and placed in a clean and dry 15 mL centrifuge tube. To ensure the removal of any residual moisture in the food wastes, it was first dried in an oven at 55 °C for 90 min to remove any potential moisture already present in food waste particle. After cooling the food waste sample back to room temperature, 15 mL of DI water was added to each centrifuge tube. The mixture was hydrated for 90 min at room temperature, estimated to be about 25 °C. The mixture was then centrifuged at 25 °C for 15 min at 9000 rpm. The supernatant was removed, and the hydrated residue (m_h) was weighed. Three samples of each food waste particle type weighed to

obtain triplicate measurements. WHC of food waste particles was measured with Eq. (1) below:

$$WHC = \frac{m_h - m_i}{m_i} \quad (1)$$

Where m_h is the mass of the hydrated sample, m_i is the initial mass of the sample.

Scanning electron microscopy of food waste particles (SEM)

The food waste particles were studied with a JEOL JSM-5500 scanning electron microscope (SEM) (JEOL, Japan) using an accelerating voltage of 5 to 20 kV. Samples were secured with double-sided carbon adhesive tape to the SEM stubs. The samples were sputter-coated with gold under an argon atmosphere for at a current of approximately 15 to 20 mA for 45 s using an auto fine JFC 1600 coater (JEOL, Japan) prior to imaging.

Rheological test

The rheological properties of the hydrogels and 3DFP inks were studied using a modular compact rheometer (Anton Paar MCR 702E

MultiDrive). To thoroughly comprehend the rheological properties, four types of rheological measurement profiles were compiled with references from several earlier works on 3DFP inks/ bioprinting inks. All measurements were conducted at a programmed temperature of 25 °C. After the sample was placed between the stage and a 25 mm parallel plate (PP25) spindle of the rheometer, the spindle was lowered to a measuring gap of 0.55 mm, and samples at the edge were trimmed prior to the start of the test. Viscosity measurements were repeated in triplicates ($n = 3$) for the different hydrogels and the 3DFP inks with different food waste percentage.

- (i) Strain sweep: Viscoelastic properties were studied with oscillatory measurements that were conducted with shear strain varying from 0.1 % to 100 % at a fixed frequency of 1 Hz. 25 data points were collected with this test profile. (Mao and Meng, 2024)
- (ii) Frequency sweep: Assessed over an angular frequency range from 0.01 to 100 rad/s at a constant strain of 1 %. 15 data points were collected with this profile. (Kim et al., 2018; Li et al., 2016)
- (iii) Flow measurement: Viscosity study carried out in a range of shear rates starting from 0.5 1/s to 500 1/s. 58 data points were collected with this measurement profile. (Zhang et al., 2022; Pant et al., 2021)
- (iv) Recovery tests measure the stress in three steps at 10 1/s (20 data points), 100 1/s (20 data points), and again at 10 1/s (20 data points). This mimics the extrusion during the printing process. (Zhang et al., 2022; Pant et al., 2021)

Food printing (3DFP) process

3DFP inks were filled into a 3 mL BD medical syringe before it was carefully transferred to a 3 mL Nordson syringe via a tip-to-tip transfer method connecting two syringe tips with a tube connector. The occurrence of large air bubbles can be reduced with this tip-to-tip transferring method, achieved by disconnecting the connecting tube between the two syringe tips from the setup to purge any large bubbles. Cellink Bio X printer was used to conduct the 3DFP process.

To study the 3DFP inks, a 2×2 cm square design (either printed with a single layer or six-layers) with a 10 or 15 % infill grid design was chosen to evaluate inconsistencies such as material gaps, slumping, and/or bleeding of the printed structures. Parameters that were adjusted include printing speed (mm/s) and printing pressure (kPa). Prior to assessing printability, a suitable nozzle size should be selected to ensure smooth extrusion of the food waste inks. The largest particle of each food waste type was evaluated for its estimated hydrated diameter (D_h) as per Eq. (5) below using volume swelling ratio (Q_v). Tabulated D_h ranged from 24 – 73 µm. Nozzle diameter is generally recommended to be at least three times wider than the largest particle especially for polydisperse particles. (Xin et al., 2021) Initial trials employed nozzles with a minimum inner diameter (ID) of 0.41 mm, with the size gradually increased based on extrusion performance. Finally, a nozzle with an inner diameter of 0.84 mm (20-gauge tapered nozzle) was selected to accommodate both particles swelling and the rheological properties of the ink.

$$Q_v = \frac{V_h}{V_d} = \frac{V_d \pm V_w}{V_d} = 1 + \frac{V_w}{V_d} \quad (2)$$

$$V_d = \frac{m_d}{\rho_d} \text{ and } V_w = \frac{m_w}{\rho_w} \quad (3)$$

$$Q_v = 1 + \frac{m_w/\rho_w}{m_d/\rho_d} = 1 + WHC \frac{\rho_d}{\rho_w} \quad (4)$$

$$D_h = D_d \times Q_v^{1/3} \quad (5)$$

Where Q_v is the volume swelling ratio, V_h is the hydrated particle volume, V_d is the volume of dry particle, V_w is the volume of water, m_w is the mass of

water, m_d is the dry mass, ρ_w is the density of water, ρ_d is the density of dry particle, D_h is the diameter of hydrated particle, D_d is the diameter of dry particle.

This swelling estimation makes several simplifying assumptions: it uses tap density as a proxy for true particle density, treats particles as isotropic spheres, and assumes all absorbed water increases internal particle volume rather than filling interparticle voids. It also presumes that hydration does not cause fragmentation, collapse, or compositional changes, and considers only equilibrium swelling without accounting for kinetics, temperature, pH, or material heterogeneity. These calculations offer a rough guide for nozzle sizing to reduce clogging risk rather than an exact prediction of particle behavior.

Extrusion parameters were optimized through a stepwise approach. Initial trials involved single-layer grids (10 % infill) using 5 % (w/v) lettuce ink at 8 mm/s, with extrusion pressure varied between 8 and 12 kPa to identify a stable pressure range. Once established, six-layer constructs with 15 % infill were printed for all samples to evaluate consistency and stacking stability. Lettuce concentration was then increased incrementally (10 %, 20 %, 30 % w/v), and only six-layer prints were performed. For each formulation, extrusion pressure was fine-tuned in 2–3 kPa steps to determine optimal flow. This protocol was applied to all food-waste inks, starting at 20 % (w/v), with concentration adjusted $\pm 10\%$ as needed.

Storage study

3DFP inks were prepared and stored at refrigeration temperature (4 °C) to study the potential rheological changes of these inks in this condition. The rheological properties were evaluated weekly for a total of four weeks.

Statistical analyses

Graphs with statistics were prepared using GraphPad Prism 10. The mean and standard deviation (SD) of triplicate measurements tabulated either with GraphPad Prism 10 or Microsoft Excel 365. Statistical analyzes were performed in Minitab 18, where one-way analysis of variance (ANOVA) was used to assess differences among groups. Results are reported as mean \pm SD, and statistical significance was defined as $p < 0.05$.

Results & discussion

Properties of food waste particles

In this study, food waste particle distributions were processed minimally to mimic real-world upcycling scenarios and to avoid addition process cost. While this may expose the study to more challenges, it would allow optimized ink formulations for practical 3DFP applications. All food waste samples (with the exception of butterhead lettuce which was first freeze-dried) were pre-processed using simple blending followed by sieving. The resulting food waste particles were then characterized for tap density, particle morphology, and water hydration capacity (WHC). SEM images revealed the morphology and size of the food waste particles, which could affect the uniformity and stability of 3DFP inks. Tap density assessed packing and flow properties, while WHC evaluated moisture retention capacity, crucial for ink storage performance and layer integrity. These characterizations guided the selection of suitable hydrogel carriers for optimal 3DFP performance by predicting how each food waste integrates with the hydrogel carrier, enhancing ink stability and printability.

SEM images at 1000 \times magnification can be found in Fig. 2, blended and freeze-dried lettuce had particle size ranging from 20 – 60 µm, while factory-processed okara was about 10 – 30 µm. Freeze-dried lettuce and okara exhibited larger flake-like structures, distinctly different from SC, which had granular shapes between 5 – 20 µm. Larger SC particles

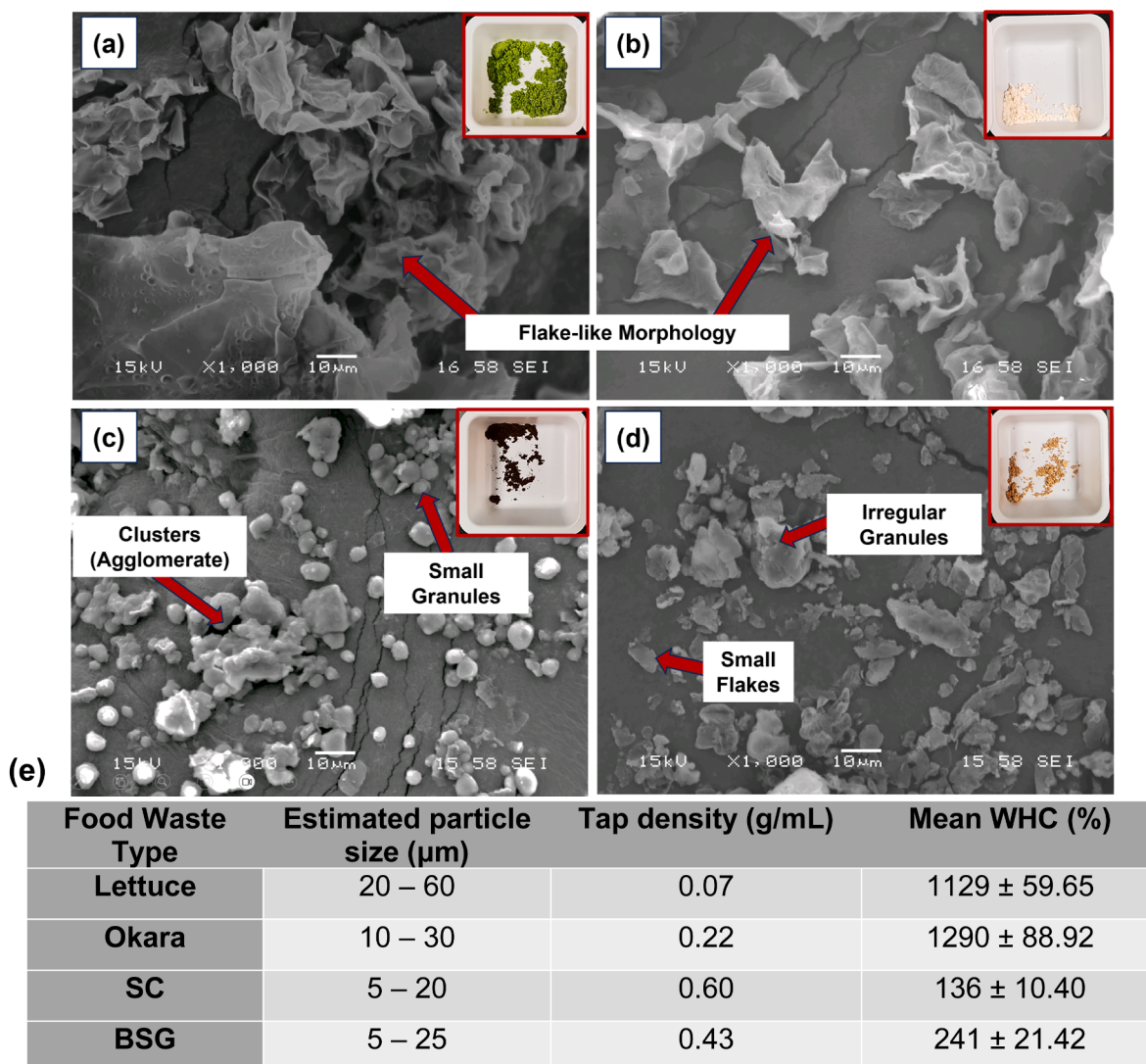


Fig. 2. SEM images (1000 \times magnification) of the four different food waste particles used in this study: (a) lettuce, (b) okara, (c) sesame cake (SC), and (d) brewer's spent grain (BSG). (e) Overview of tap density and water hydration capacity (WHC) measurement results for the food waste particles.

appeared as clusters of granules adhered together. BSG had a mix of smaller flakes and irregular fragments, with sizes ranging from 5 – 25 μm . Variations in particle shape and size were likely due to differences in material hardness and factory grinding methods.

The overview data of the tap density and mean WHC % can be found in Fig. 2(e). Freeze-dried lettuce had the lowest tap density of 0.07 g/mL, while SC had the highest tap density of 0.6 g/mL, nearly ten times greater. Tap density depends greatly on particle shape, size, and structure, affecting packability. Freeze-dried lettuce's low tap density is attributed to its initial high-water content in the vegetable and large flake sizes, reducing packability compared to smaller, granular particles. Tap density insights aid in understanding rheological behavior and storage stability.

WHC evaluation tabulated in Fig. 2(e) showed okara with the highest WHC, followed by freeze-dried lettuce, as they have hydrophilic compositions and moisture retention abilities. For instance, okara's WHC is attributed to its soy protein isolate, composed of >50 % hydrophilic amino acids, and its high dietary fiber, (Fu et al., 2017; Castro-Criado et al., 2023) which forms hydrogen bonds with water. (Chaplin, 2003) In contrast, BSG and SC exhibited lower WHC values. Detailed discussion on the impact of WHC is presented under section "Rheological properties of 3DFP inks and their printing performance". WHC study is critical for optimizing 3DFP ink formulations, as it affects consistency and

stability. Flake-shaped particles with higher surface area enhance interactions with hydrogels and other flakes, increasing friction or interlocking. (Wypych, 2016) Additionally, particle density impacts rheological properties and the amount of waste that can be incorporated into 3DFP inks. WHC strongly influences the rheology and long-term stability of 3DFP inks during storage.

Rheological properties of hydrogel candidates

In this study, we considered three common hydrogels to be used as base gel carriers in blending with food waste: alginate, KC, and TPS starch. While alginate and KC are well-established candidates for 3DFP, (45,46) TPS remains underexplored, as research has more commonly focused on gelatinized starch. However, TPS plasticized with glycerol is known to exhibit enhanced flexibility and mechanical strength potentially improving printing outcome, hence TPS was included in this hydrogel test matrix. (Marcin and Leszek, 2009) Rheological assessments of all hydrogels were conducted in triplicates to assess their suitability for blending with the food wastes, and a summary of the results can be found in Fig. 3.

Rheological measurements of the hydrogels were conducted within three days post-preparation to minimize variations in viscosity over time. Dynamic viscosity measurements captured viscosity at different

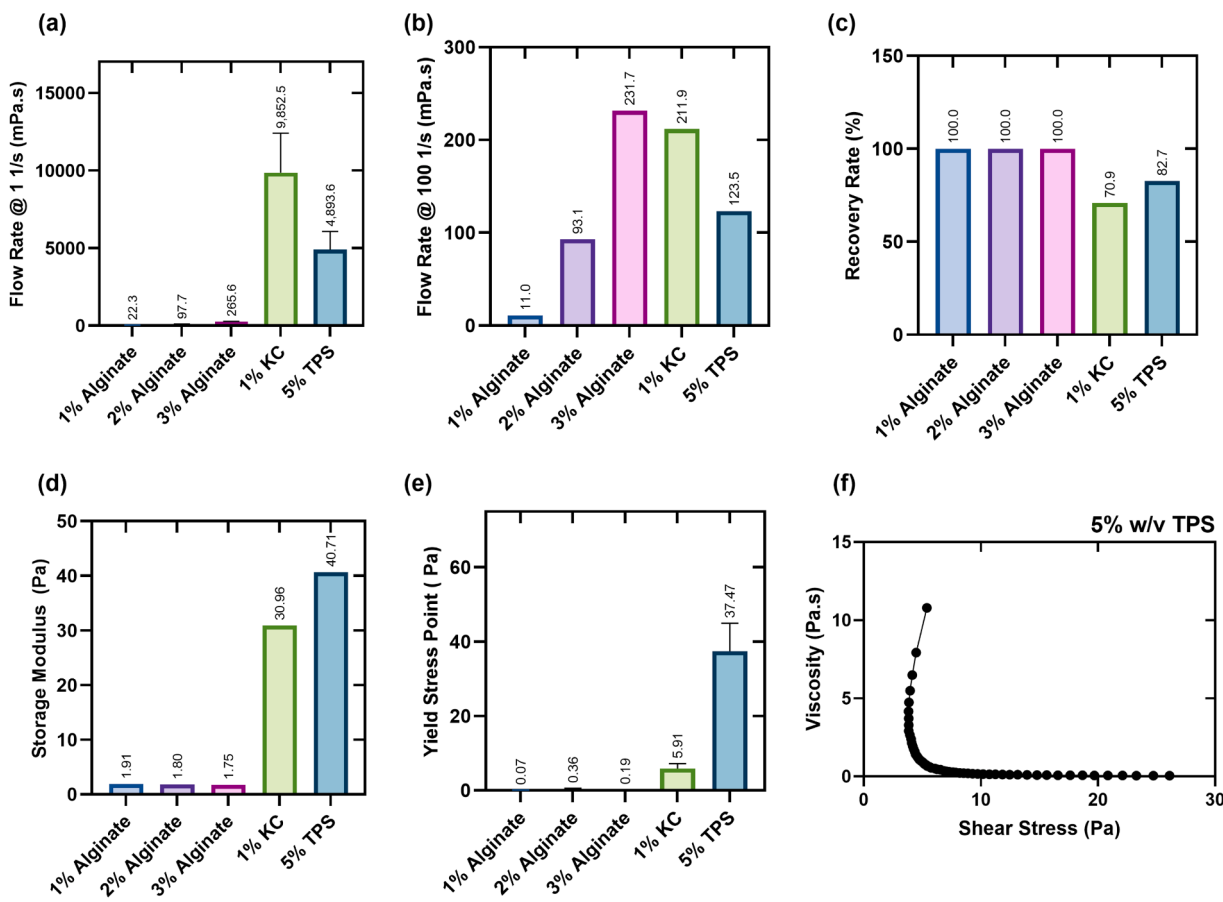


Fig. 3. Summary of rheological measurements for all hydrogels: (a, b) dynamic viscosity at shear rates 1 and 100 1/s, (c) recovery rate, (d, e) amplitude sweep results, showing storage modulus, yield stress, and (f) a viscosity – shear stress curve of 5 % w/v TPS demonstrating shear-thinning behavior. Each dataset in (a)–(e) was evaluated with $n = 3$, with standard deviations represented by the error bars.

flow rates, 1 1/s and 100 1/s were selected for comparison of the different hydrogels, as shown in Fig. 3(a) and Fig. 3(b). As anticipated, flow rate measurements at both 1 1/s and 100 1/s showed a significant increase ($p < 0.05$) with alginate percentage. All the hydrogels tested displayed shear-thinning properties (Fig. 3(f) and Figure S1), making them suitable for extrusion via 3DP. The recovery rate of 3DFP inks was assessed to understand the hydrogel performance, results ranged from 70 % to 100 % (Fig. 3(c)). This confirms their suitability for 3D food printing by ensuring structural integrity post-extrusion.

In Fig. 3(d), storage modulus obtained from amplitude sweep is critical in determining elastic properties. From the results we find better elastic properties from only 1 % w/v KC and 5 % w/v TPS. Furthermore, both amplitude sweep, and frequency sweep of all alginate gels (Figure S2 – S5) revealed unstable readings at low strain and low frequencies across all three alginate samples, followed by crossover of storage modulus (G') and loss modulus (G''), as shown in Table S1 in Supplementary Data. The result indicates $G'' > G'$ at both low strain and frequencies, suggesting that alginate predominantly exhibits viscous behavior rather than elastic stability. Within the context of 3DP, this implies poor shape retention, where the printed structure may lack mechanical integrity and spread post-deposition. The absence of a crosslinker could lead to this phenomenon as unmodified alginate hydrogels lack sufficient intermolecular interactions to maintain a solid-like structure. This aligns with previous studies where alginate is often blended with stronger gel-forming biopolymers or reinforced with calcium-based crosslinkers post-printing to improve mechanical stability. (Shi, 2019; Rysenaer et al., 2023)

In contrast both 1 % w/v KC and 5 % w/v TPS demonstrated consistently higher G' than G'' (Figure S1, S6 – S9, Table S1), indicating

dominant elastic behavior and greater structural stability for 3D printing application. Another important parameter to assess 3D printability is the loss factor ($\tan \delta$). $\tan \delta$ is defined as ratio between storage and loss modulus (G''/G'), and it measures the balance between elasticity and viscosity. (Jergitsch et al., 2023) Studies suggest that a $\tan \delta$ between 0.2 – 0.7 is optimal for 3D printing process although this can vary depending on the 3D printer utilized. (Shi, 2019; Herrada-Manchón et al., 2023) Unfortunately, reliable $\tan \delta$ values for the three alginate hydrogels could not be derived from this data due to the huge fluctuation as mentioned. In KC and TPS, the mean value was 0.34 and 0.35 respectively, suggesting that these materials may be better suited for maintaining structural integrity in 3D-printed layers.

Consequently, alginate hydrogels were not considered as the primary base carrier for food waste incorporation. Instead, 1 % w/v KC and 5 % w/v TPS were selected as the most suitable candidates for further formulation trials using the freeze-dried butterhead lettuce. As shown in Fig. 3(a), both KC and TPS exhibited extremely high viscosities at low shear rates, indicating their gel-like nature and suggesting that higher extrusion pressure may be required. However, their pronounced shear-thinning behavior is advantageous, allowing the inks to flow smoothly through the nozzle while rapidly recovering viscosity after deposition and thus preserving structural integrity. These are key qualities that make them well-suited for 3D food-printing (3DFP) applications.

Iterations to optimize properties using freeze-dried lettuce agricultural waste

Freeze-dried lettuce was selected for initial evaluation due to its highly hygroscopic nature, low tap density, and large flake-like

morphology. These characteristics result in a high volume-to-mass ratio and can complicate the blending process, while also presenting additional challenges during extrusion-based 3DFP. As such, freeze-dried lettuce was anticipated to be the most difficult food waste material to incorporate effectively into hydrogel-based inks, making it an ideal candidate for iterative evaluation before testing other food waste sources. Such an iterative step-by-step methodology has also been demonstrated in the designing of other 3D printing food ink formulations. (Kim et al., 2018; Rodríguez-Herrera et al., 2024; Molina-Montero et al., 2023)

With the selected 1 % w/v KC and 5 % w/v TPS hydrogels, the gradual addition of food waste was predicted to add stiffness, improving layer stability. (Molina-Montero et al., 2023) The rheological comparisons were made between the 1 % w/v KC and 5 % w/v TPS after they were blended with 5 % w/v lettuce to determine the better suited hydrogel type to proceed with the experiments. Both 3DFP lettuce inks exhibited gel-like properties with higher storage modulus (G') than loss modulus (G''). 1 % w/v KC with 5 % w/v lettuce had a viscosity of 659.6 mPa.s, while 5 % w/v TPS with 5 % w/v lettuce had a viscosity of 1555.8 mPa.s. The recovery rate was significantly affected by the addition of lettuce. The 1 % w/v KC with 5 % w/v lettuce had a much lower recovery rate of only 10.1 %, whereas the 5 % w/v TPS with 5 % w/v lettuce demonstrated a significantly better recovery rate of 88.9 %. 5 % w/v TPS was selected as the hydrogel to move forward as: (i) the trial with 5 % w/v lettuce food waste showed a better recovery rate, (ii) TPS is more robust for processing since KC starts softening at temperatures around 30 °C, potentially compromising the printed structure if further heating or cooking is required. (Wypych, 2016)

The freeze-dried lettuce, characterized by its flake-like structure (in Fig. 2(a)), along with the use of TPS gel, ensured the maintenance of printing layer integrity without noticeable slump post-printing. As shown in Fig. 4, the printing evaluation started from 5 % w/v lettuce 3DFP ink slowly moving to 10 % w/v to establish the pressure range required. Before moving on to 10 % - 30 % w/v lettuce 3DFP inks, it was necessary to increase the pressure and reduce the printing speed with

increasing lettuce load. Notably, at a 30 % w/v lettuce composition, the ink showed signs of drying out, leading to poor substrate adhesion and undesired ink displacement, as per Fig. 4(e).

However, reducing the printing speed from 6.5 mm/s to 5.5 mm/s effectively mitigated this issue, facilitating the production of a more structured grid pattern, as shown in Fig. 4(f). Additionally, each print was assigned a printability score from 1 to 5 based on visual quality and structural integrity, with 5 representing flawless prints and 1 indicating failed or collapsed structures.

Out of all the different lettuce loads, 20 % w/v achieved the best printability with maximum incorporation of freeze-dried lettuce while maintaining stable printing layers and minimal impact on printing speed. Hence, based on the findings of this study, a 20 % w/v food waste composition was selected as the initial formulation for all subsequent food waste evaluations. This preliminary iterative study provides an initial understanding of freeze-dried lettuce as a 3D printing food ink. It establishes a benchmark with a 20 % w/v starting point for extending the approach to other food waste materials. Since the study was not designed for robust prediction or modeling, future work can look at increasing the number of experimental runs to enable the application of advanced statistical analyses.

Rheological properties of 3DFP inks

Fig. 5 summarizes all rheological properties of 3DFP inks prepared with 10 % w/v okara, then 20 % w/v and 30 % w/v for lettuce, BSG and SC. For SC and BSG, the food waste incorporation percentages were determined based on an optimization study using lettuce, which identified 20 % w/v as the optimal concentration range for achieving printability and structural stability. An interesting observation was that while all three food inks formulated with 20 % w/v and 30 % w/v food waste exhibited a significant increase in storage modulus (Fig. 5(c)), $p < 0.05$ for 30 % w/v when compared to 20 % w/v. However their viscosity at 100 1/s (Fig. 5(a)) showed no significant difference. This suggests that despite the higher solid content, the inks retained good shear-

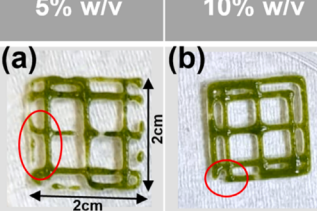
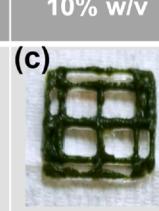
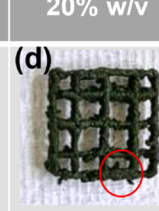
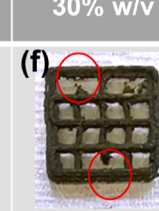
3DFP Ink (Lettuce)	5% w/v	10% w/v	10% w/v	20% w/v	30% w/v	30% w/v
Top view	(a) 	(b) 	(c) 	(d) 	(e) 	(f) 
Infill percentage/ No. of layers	10% 1 layer	10% 1 layer	10% 6 layers	15% 6 layers	15% 6 layers	15% 6 layers
Printing pressure/ Printing speed	8 kPa 8.0 mm/s	12 kPa 8.0 mm/s	20 kPa 8.0 mm/s	85 kPa 7.0 mm/s	150 kPa 6.5 mm/s	160 kPa 5.5 mm/s
Printability Score	4	4	4	4.5	1	3
Remarks/ Observations (Missing detail, inconsistent print, ink bleed out are circled in red)	<ul style="list-style-type: none"> Able to print smoothly Some missing details 	<ul style="list-style-type: none"> Relatively good consistency A missing detail in the corner 	<ul style="list-style-type: none"> Slightly inconsistent in printed lines No missing details 	<ul style="list-style-type: none"> Stable printed layers Some tailing effect from ink 	<ul style="list-style-type: none"> Ink was too dry and was unable to stay in place well with printing speed 	<ul style="list-style-type: none"> Able to print relatively stable layers Several missing details

Fig. 4. 3DFP inks with varying lettuce compositions and corresponding observations, the red circle on the top view images show various printing inconsistency including missing detail, inconsistent print, tailing are circled in red: (a) A single-layer print with 5 % w/v lettuce was achieved, (b, c) 10 % w/v lettuce enabled consistent printing, (d) 20 % w/v lettuce produced stable prints with slight tailing, (e, f) 30 % w/v lettuce allowed a six-layer print but required higher extrusion pressure and showed some loss of fine details.

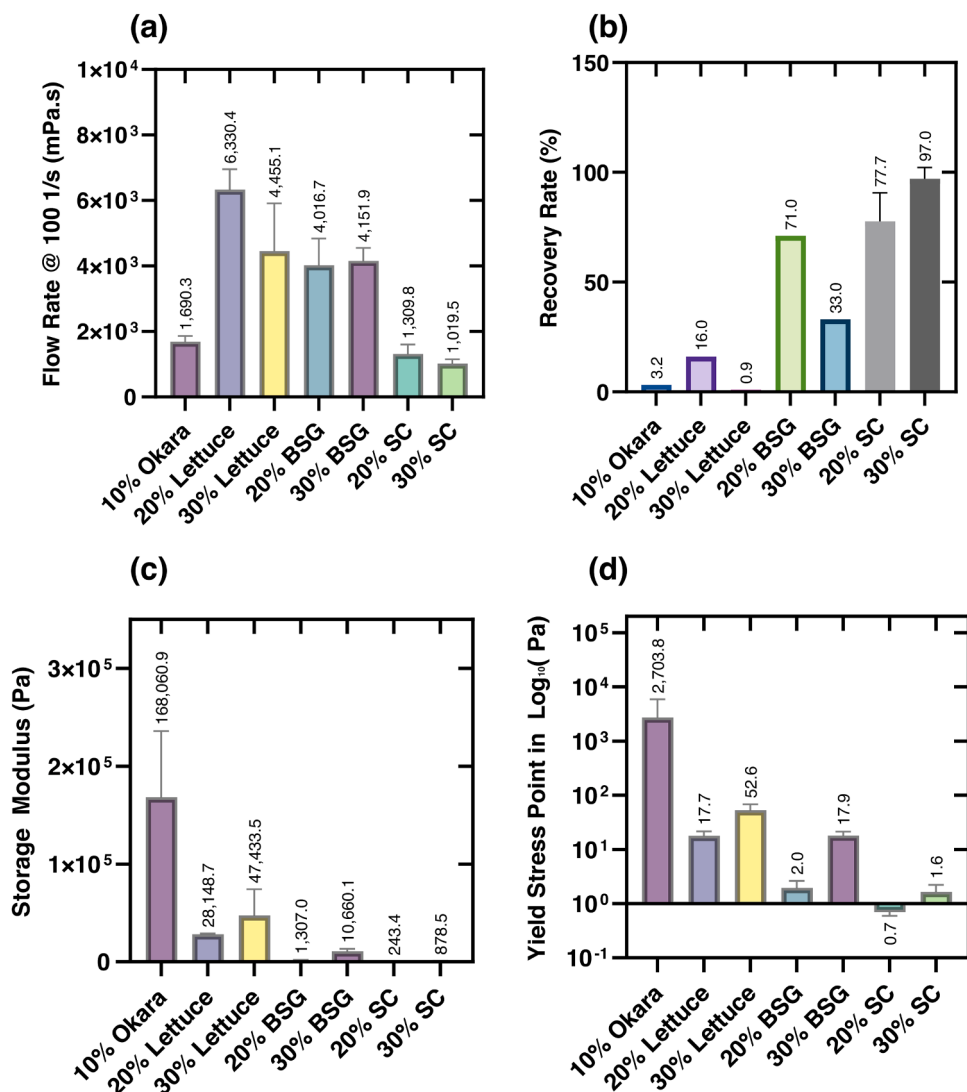


Fig. 5. Summary of rheological measurements for all 3DFP inks: (a) dynamic viscosity at shear rate 100 1/s looking at extrudability, (b) looked at the recovery rate of the 3DFP inks, (c) storage modulus from amplitude sweep, and (d) yield stress point from amplitude sweep looking at minimal stress required to initiate flow in a material. Each dataset in (a)–(d) was evaluated with $n = 3$, with standard deviations represented by the error bars.

thinning behavior (Figure S10), allowing extrusion with minimal additional pressure while maintaining well-defined printed layers.

Another general trend observed was that increasing the food waste percentage significantly increased the yield stress point (Fig. 5(d)) while reducing the recovery rate (Fig. 5(b)) in lettuce and BSG 3DFP inks ($p < 0.05$). The yield stress increased with higher food waste incorporation due to particle interactions, resulting in stiffer material. The reduction in recovery rate with increasing food waste percentage was expected for several reasons. Recovery rate is primarily influenced by the hydrogel carrier recovering the internal broken polar bonds; (Habib and Khoda, 2022) as the food waste content increases, the proportion of hydrogel decreases, thus reducing the material's ability to regain its original structure after shear deformation.

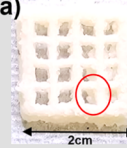
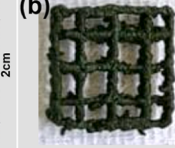
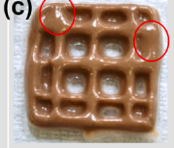
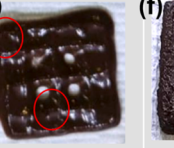
For okara, the initial trial was to prepare 20 % w/v inks following the percentage of all other 3DFP inks mentioned. However, it was drying out quickly and challenging to print, hence the percentage had to be reduced to only 10 % w/v. Even at 10 % w/v okara 3DFP ink continued to exhibit the highest storage modulus and yield stress point as shown in (Fig. 5(c)) and (Fig. 5(d)). While a high storage modulus can enhance the stability of 3D-printed layers post-printing, excessively high values may compromise extrudability, as increased rigidity makes extrusion more challenging. Additionally, rheological measurements at higher shear rates

led to large chunks of 10 % w/v okara 3DFP ink to be displaced between the measurement plates, indicating potential measurement inaccuracies.

Given the high viscosity of okara-based ink, a larger PP50 (50 mm) plate may be necessary to ensure better sample distribution and minimize edge effects. The displacement observed when using a PP25 (25 mm) plate in this set of experiments resulted in gaps left by displaced okara inks and reduced friction, leading to underestimated viscosity readings of okara 3DFP ink as shown in Fig. 5(a). This issue is further confirmed by 3DP trials, where 10 % w/v okara ink required the highest extrusion pressure of 140 kPa during 3D printing (Fig. 6(a)). The need for such high printing pressure suggests that the actual viscosity of 10 % w/v okara ink is higher than measured. With okara's high WHC, and flake-like particle morphology which increases surface area, this can contribute to particle swelling, increasing viscosity and rigidity of ink. To improve extrudability, future studies should explore blending okara with a lower viscosity hydrogel to achieve a more workable and printable consistency.

Printing performance of 3DFP inks

Rheological evaluation is essential for establishing a benchmark and gaining a fundamental understanding of the material's potential

3DFP Ink	10% w/v Okara	20% w/v Lettuce	20% w/v BSG	30% w/v BSG	20% w/v SC	30% w/v SC
Top view	(a) 	(b) 	(c) 	(d) 	(e) 	(f) 
Viscosity @ 100 1/s (Pa)	1,690.3 ± 174.3	6,330.4 ± 626.5	4,016.7 ± 819.4	4,151.9 ± 398.9	1,309.8 ± 297.7	218.3 ± 60.9
Yield Stress Point (Pa)	2703.8 ± 3157.9	17.7 ± 3.9	2.0 ± 0.7	17.9 ± 3.3	0.7 ± 0.1	1.63 ± 0.6
Storage Modulus (Pa)	$1.7 \times 10^5 \pm 6.8 \times 10^4$	$2.8 \times 10^4 \pm 900.1$	$1,307.0 \pm 477.0$	$1.1 \times 10^4 \pm 2.72 \times 10^3$	243.4 ± 112.9	878.5 ± 158.0
Infill percentage/ No. of layers	15% 6 layers	15% 6 layers	15% 6 layers	15% 6 layers	15% 6 layers	15% 6 layers
Printing pressure/ Printing speed	140 kPa 6.5 mm/s	85 kPa 7.0 mm/s	85 kPa 6.0 mm/s	120 kPa 7.0 mm/s	12 kPa 7.0 mm/s	85 kPa 6.0 mm/s
Printability Score	3	4.5	4	5	3	2
Remarks/ Observations (Missing detail, inconsistent print, ink bleed out are circled in red)	<ul style="list-style-type: none"> High printing pressure required Printing lines are less defined with inconsistency 	<ul style="list-style-type: none"> Stable printing layer Some tailing effect from ink 	<ul style="list-style-type: none"> Ink appear to be very flowy Ink bleed out of the printed grid structure 	<ul style="list-style-type: none"> Can print consistently and print out has smooth lines. Grid shape slightly distorted due to printing speed 	<ul style="list-style-type: none"> Very inconsistent printing Several missing grid from ink bleeding. Nozzle appears clogged after 1 layer. 	<ul style="list-style-type: none"> Similarly inconsistent printing as per 20% w/v SC. Printability is not repeatable as the nozzle is often clogged.

**In the 10 % w/v okara sample, the rheological measurements may be inaccurate due to large chunks of the ink being expelled, reducing contact between the material and the measurement plate. Furthermore, only two measurements were feasible, making n = 2 for this sample.

Fig. 6. Overview of the printing performance of various 3DFP inks and their key rheological properties, the red circle in the top view images show various printing inconsistency including ink bleed out of the grid detail and tailing: (a) 10 % w/v okara 3DFP ink, (b) 20 % w/v lettuce 3DFP ink, (c) 20 % w/v BSG 3DFP ink, (d) 30 % w/v BSG 3DFP ink, (e) 20 % w/v SC 3DFP ink, and (f) 30 % w/v SC 3DFP ink.

**In the 10 % w/v okara sample, the rheological measurements may be inaccurate due to large chunks of the ink being expelled, reducing contact between the material and the measurement plate. Furthermore, only two measurements were feasible, making n = 2 for this sample.

printability in 3D food printing. Several factors could influence the rheology, for instance, the tested properties of WHC, particle size morphology, its density, and food composition. Fig. 6 provides a compilation of the printing performance along with key rheological measurement data. As mentioned, 10 % w/v okara ink which has the highest yield stress point and storage modulus was the hardest to extrude. That said, while the 20 % w/v and 30 % w/v SC 3DFP ink had the lowest yield stress point and storage modulus, it did not immediately become easier to dispense (Fig. 6(e) and (f)). The 3DFP ink of SC had printing outcome that was highly inconsistent as the nozzle often got stuck after printing the first layer. The clogging issue could be caused by clusters of SC particles as shown in SEM images in Fig. 2(c), moreover the hydrophobicity with its high fat content may also affect the surface tension between particles (Xu et al., 2013) leading to such clustering effect.

In contrast to 10 % w/v okara, 20 % w/v SC, and 30 % w/v SC 3DFP inks, the parameters for lettuce and BSG inks were easier to finetune, the 20 % w/v BSG ink appeared runny and some grid gaps disappeared under inks that has bled out (Fig. 6(c)), while 30 % w/v SC ink required a higher printing pressure but the printed layer remained very stable with no flow out, even when left at room temperature on the lab bench for 30 min after printing (Fig. 6(d)).

Beyond rheological behavior, the composition of food waste can directly influence the nutritional value of 3D-printed food for consumers and also plays a crucial role in printability. The nutritional composition of the food wastes used in this study has been characterized separately in a publication by our research group member – Yu et al. (Yu et al., 2024). For instance, okara, which has the highest combined crude fiber and carbohydrate content, exhibits the highest WHC. This results in a highly stiff and "dry" 3D printing ink at 10 % w/v concentration, making it unstable for rheological measurements. Crude fiber, primarily composed

of hydrophilic polysaccharides such as cellulose and hemicellulose, increases WHC and imparts stiffness due to its long-chain molecular structure. Similarly, hydrophilic carbohydrates further contribute to this effect, reinforcing the material's water-retention properties and printability challenges. BSG has similar crude fiber content but lower carbohydrates, resulting in moderate WHC, lower viscosity, improving its 3D printability comparatively.

For freeze-dried butterhead lettuce, Sular et al. suggest its crude fiber and carbohydrate content constitute ~50 % of its dry matter, (Sularz et al., 2020) which would contribute to its higher viscosity and WHC. Despite that, freeze-dried lettuce mixed well with TPS to form a stable 20 % w/v 3DFP ink. The differences in tap density and composition between lettuce and okara significantly affect their rheological behavior. SC on the other hand, with its granular, high-density particles, caused frequent clogging, leading to inconsistent layers. The presence of agglomerates in the SEM image (Fig. 2(d)) contributed to needle clogging during 3DFP. Additionally, SC has the lowest carbohydrate content, along with lower WHC and viscosity. With the highest fat content among all tested food wastes, it is likely to exhibit increased hydrophobicity, which may have contributed to the lowest yield stress point observed (Fig. 6(f)), even at a 30 % w/v concentration.

Repeatability, storage stability and multi-material printability of these 3DFP inks

Using flow viscosity at a shear rate of 100 1/s and storage modulus as the key rheological indicators, the stability of four selected 3DFP inks – 10 % w/v okara, 20 % w/v lettuce, 20 % w/v SC, and 20 % w/v BSG stored at 4 °C were quickly assessed for their rheological stability over four weeks. The results, including day one (referred to as week 0), are recorded in Fig. 7. In terms of dynamic viscosity at 100 1/s shear rate,

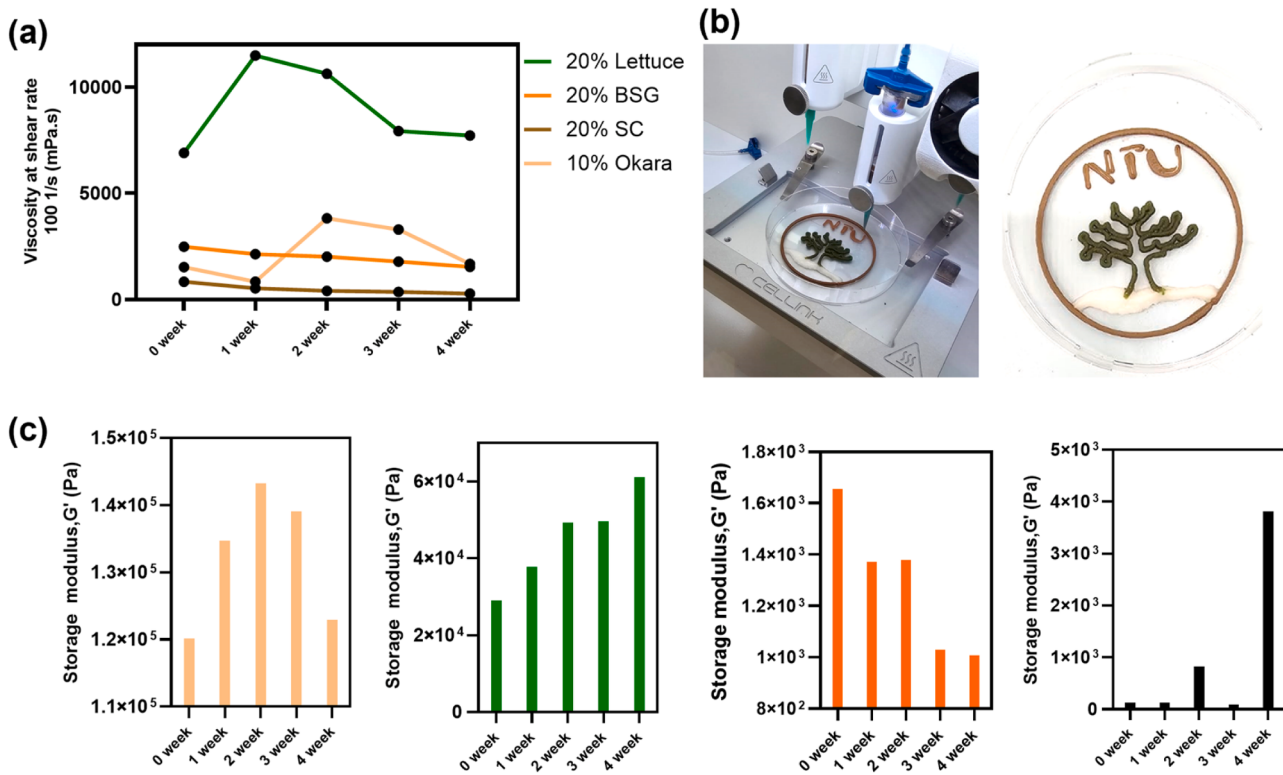


Fig. 7. Storage stability of all 3DFP inks were assessed over four weeks (a) all 3DFP inks were measured for their flow viscosity at 100 1/s data, (b) Multi-ink print trial using a five-layer design with Cellink Bioprinter. 20 % w/v BSG ink was used for the circular outline and the word "NTU," 20 % w/v lettuce ink was used to 3D print the tree design, and 10 % w/v okara ink was used to print the wavy baseline beneath the tree. (c) Storage modulus of 10 % w/v Okara, 20 % w/v lettuce, 20 % w/v BSG, and 20 % w/v SC.

both the 20 % w/v BSG and 20 % w/v SC inks showed a steady decline in viscosity over the four weeks. 10 % w/v okara 3DFP ink was evaluated but as mentioned earlier, the results are unlikely to be accurately represent the actual viscosity in this particular study and should be reassessed again in future work.

Visual observations of the 3DFP inks in storage showed that SC separated from the hydrogel due to its high density of 0.6 g/mL, which is the highest among all food wastes. Its low WHC of 10.40 % w/v contributed to this separation, as the SC food particles could not remain homogeneous with the hydrogel. Viscosity of the 20 % w/v SC ink dropped significantly from 835.4 mPa·s to 277.2 mPa·s by the final week, demonstrating this potential separation (Fig. 7(a)). The 20 % w/v BSG ink (Fig. 7(a)) showed a similar trend, with viscosity decreasing gradually from 2480.5 mPa·s to 1532.5 mPa·s over four weeks, however without visible particle separation from the hydrogel.

The 20 % w/v lettuce ink (Fig. 7(a)) experienced a sharp viscosity increase after seven days, followed by a gradual decline and a further drop to around 7000 mPa·s from the third week. Unlike SC, which has low WHC and is more hydrophobic, lettuce has a high WHC second to okara. The hydrophilic nature of lettuce likely caused the initial viscosity increase, followed by a viscosity decline due to particle degradation, as indicated by a color change from bright green to dark olive green. The lack of preservatives in the formulated 3DFP inks may contribute to this degradation and the resulting changes in rheological behavior. These rheological changes are further supported by time-resolved measurements of the storage modulus (G'), which reflect the elastic integrity of the hydrogel network. For instance, the steady decline in G' for SC and BSG inks (Fig. 7(c)) corresponds to weakening polymer-particle interactions, while the temporary increase in G' for lettuce and okara suggests transient stiffening caused by water redistribution and swelling before degradation dominates.

Apart from storage stability evaluation, repeatability of different

3DFP inks batches was also assessed by comparing their flow viscosity at shear rate of 100 1/s (Figure S11). Among the samples, 20 % (w/v) lettuce ink exhibited the highest mean viscosity (6330 mPa·s) with a relatively low standard deviation (± 626 mPa·s), indicating consistent flow behavior across batches. The 20 % BSG ink showed a moderate mean viscosity (3369 mPa·s) but with higher variability (± 1067 mPa·s), suggesting slight batch-to-batch inconsistency, while the 20 % SC ink had the lowest viscosity (1204 mPa·s) among the tested samples, with a standard deviation of ± 414 mPa·s, reflecting moderate repeatability. For the 10 % okara ink, only one data point could be obtained due to unstable rheological properties as mentioned in earlier sections. These findings highlight the 20 % w/v lettuce 3DFP ink as the most rheologically stable candidate.

To conclude the study, multi-ink 3D printing was conducted using a five-layer design to evaluate the printability of 10 % w/v Okara, 20 % w/v BSG, and 20 % w/v lettuce 3DFP inks. The 20 % w/v SC ink was excluded from this trial due to poor printing performance. In this trial, 20 % w/v lettuce ink was used to print the tree outline (in Fig. 7(b), as a symbol of sustainability), 20 % w/v BSG ink was used for the circular outline, and the word "NTU" (our institution), and 10 % w/v okara ink was used to print the wavy baseline beneath the tree design. The 20 % w/v lettuce ink demonstrated the best printability, followed by the 20 % w/v BSG ink, which showed only minimal tailing effects. In contrast, the 10 % w/v okara ink which was previously found to be challenging to assess exhibited the least consistent performance. The superior performance of the 20 % w/v lettuce ink and 20 % w/v BSG ink prepared with 5 % w/v TPS highlights their potential to be explored in 3DFP inks.

Conclusion

This study comprehensively examined the rheological properties of various hydrogels and their suitability as carriers for 3DFP inks

incorporating homogeneous food factory byproducts and agricultural surplus which is frequently treated as food waste. Among the tested formulations, 5 % w/v TPS demonstrated the most favorable gel-like behavior, exhibiting sufficient stiffness and elasticity, making it the most promising candidate for 3DFP applications. These food waste particles significantly influenced the rheology and printability of the inks. Lettuce- and BSG-based inks at 20 % w/v composition, prepared with TPS, exhibited optimal viscosities of 4016.7 mPa·s and 6330.4 mPa·s at 100 1/s shear rate, respectively. Both inks produced consistent printing layers, indicating their rheological suitability for 3DFP. However, additional factors such as storage modulus, yield stress, and hydrogel-food waste interactions must also be considered. SC-based inks, despite having low viscosity, exhibited high tap density (0.6 g/mL), leading to nozzle clogging due to particle agglomeration and phase separation. Okara-based inks, with their high WHC of 1290 %, resulted in a viscous, dry ink, requiring a reduced concentration of 10 % w/v for improved printability but remaining less stable overall. Storage tests revealed that 20 % w/v BSG-based inks demonstrated the highest stability, maintaining consistent viscosity over four weeks. In contrast, SC-based inks degraded rapidly due to phase separation between SC particles and TPS hydrogel, while lettuce-based inks exhibited viscosity fluctuations after two weeks, likely due to the breakdown of hydrophilic components. These findings highlight the importance of tailoring hydrogel formulations to accommodate the unique rheological properties of different food waste particles. This study leveraged the potential of 3DFP to valorize these edible manufacturing food byproducts, promoting sustainability and resource efficiency. Future research could focus into further optimizing formulations by evaluating hydrogel-food waste compatibility of okara and SC, exploring different food waste combinations to achieve nutritionally balanced ink formulations. For instance, sesame cake (SC) could be incorporated in lower percentages to enhance flavor complexity while minimizing printability issues. Additionally, efforts should be directed toward detailed nutritional composition, evaluation of the texture profile, and sensory-perception physicochemical properties, ensuring food safety, and scaling up 3DFP for sustainable food production.

Ethic statement

This study did not involve human participants or animal subjects. All experimental procedures were conducted in accordance with ethical guidelines for material-based research. No ethical approval was required.

CRediT authorship contribution statement

Ling Xin Yong: Writing – original draft, Supervision, Project administration, Methodology, Investigation, Formal analysis, Data curation, Conceptualization. **Xin Ying Fiona Lim:** Resources, Formal analysis, Conceptualization. **Say Chye Joachim Loo:** Writing – review & editing, Supervision, Funding acquisition.

Declaration of competing interest

The authors declare that they have no known competing financial interests or personal relationships that could have appeared to influence the work reported in this paper.

Acknowledgements

The authors would like to acknowledge V-Plus Agritech Pte Ltd, Starbucks Coffee Singapore Pte Ltd, Oh Chin Hing Sesame Oil Factory, Super Bean International Pte Ltd, and Par International Pte Ltd for providing the food waste materials used in this study. Sincere thanks are extended to Prof. Ng Kee Woei and Dr. Archana Gautam from the School of Materials Science and Engineering for granting access to the BioX

Cellink 3D printer. The authors also wish to thank the Singapore Centre for 3D Printing (SC3DP), particularly Prof. Paulo Bartolo, Dr. Bo Yang, Dr. Cian Vyas, and Ms. Yufei Cui, for their training and technical support in the use of the Cellink Bio X6 Advanced Extrusion 3D Bioprinter for multi-ink printing assessments. This work was supported by the Singapore Food Agency (SFS_RND_SUFP_001_06, NRF-SFSRND2RT-0002) and the Ministry of Education (RG79/22, RG29/24, MOE-T2EP30223-0001).

Supplementary materials

Supplementary material associated with this article can be found, in the online version, at [doi:10.1016/j.fufo.2025.100682](https://doi.org/10.1016/j.fufo.2025.100682).

Data availability

Supplementary Data.

References

- Al-Baari, A.N., Legowo, A.M., Rizqati, H., Widayat, Septianingrum, A., Sabrina, H.N., Arganis, L.M., Saraswati, R.O., Mochtar, R.C.P.R., 2018. Application of iota and kappa carrageenans to traditional several food using modified cassava flour. IOP Conf. Ser. Earth Env. Sci. 102, 012056. <https://doi.org/10.1088/1755-1315/102/1/012056>.
- Amoriello, T., Mellara, F., Galli, V., Amoriello, M., Ciccoritti, R., 2020. Technological properties and consumer acceptability of bakery products enriched with brewers' Spent grains. Foods 9 (10), 1492. <https://doi.org/10.3390/foods9101492>.
- Asghar, A., Afzaal, M., Saeed, F., Ahmed, A., Ateeq, H., Shah, Y.A., Islam, F., Hussain, M., Akram, N., Shah, M.A., 2023. Valorization and food applications of Okara (Soybean Residue): a concurrent review. Food Sci. Nutr. 11 (7), 3631–3640. <https://doi.org/10.1002/fsn3.3363>.
- Baiano, A., 2022. 3D Printed foods: a comprehensive review on technologies, nutritional value, safety, consumer attitude, regulatory framework, and economic and sustainability issues. Food Rev. Int. 38 (5), 986–1016. <https://doi.org/10.1080/8759129.2020.1762091>.
- Castro-Criado, D., Jiménez-Rosado, M., Perez-Puyana, V., Romero, A., 2023. Soy protein isolate as emulsifier of nanoemulsified beverages: rheological and physical evaluation. Foods 12 (3), 507. <https://doi.org/10.3390/foods12030507>.
- Chakraborty, I., N, P., Mal, S.S., Paul, U.C., Rahman, Md.H., Mazumder, N., 2022. An insight into the gelatinization properties influencing the modified starches used in food industry: a review. Food Bioproc. Tech. 15 (6), 1195–1223. <https://doi.org/10.1007/s11947-022-02761-z>.
- Chaplin, M.F., 2003. Fibre and water binding. Proc. Nutr. Soc. 62 (1), 223–227. <https://doi.org/10.1079/PNS2002203>.
- Chauhan, C., Dhir, A., Akram, M.U., Salo, J., 2021. Food loss and waste in food supply chains: A systematic literature review and framework development approach. J. Clean. Prod. 295, 126438. <https://doi.org/10.1016/j.jclepro.2021.126438>.
- Escalante-Aburto, A., Trujillo-de Santiago, G., Alvarez, M.M., Chuck-Hernández, C., 2021. Advances and prospective applications of 3D food printing for health improvement and personalized nutrition. Compr. Rev. Food Sci. Food Saf. 20 (6), 5722–5741. <https://doi.org/10.1111/1541-4337.12849>.
- Farcas, A.C., Socaci, S.A., Chiș, M.S., Pop, O.L., Fogaras, M., Păucean, A., Igual, M., Michiu, D., 2021. Reintegration of brewers spent grains in the food chain: nutritional, functional and sensorial aspects. Plants 10 (11), 2504. <https://doi.org/10.3390/plants10112504>.
- Feng, C., Zhang, M., Bandari, B., Ye, Y., 2020. Use of potato processing by-product: effects on the 3D printing characteristics of the yam and the texture of air-fried yam snacks. LWT 125, 109265. <https://doi.org/10.1016/j.lwt.2020.109265>.
- Fu, Z., Wu, M., Han, X., Xu, L., 2017. Effect of Okara dietary Fiber on the properties of starch-based films. Starch - Stärke 69 (11–12). <https://doi.org/10.1002/star.201700053>.
- Gudjónsdóttir, M., Napitupulu, R.J., Petty Kristinsson, H.T., 2019. Low field NMR for quality monitoring of 3D printed surimi from cod by-products: effects of the PH-shift method compared with conventional washing. Magn. Reson. Chem. 57 (9), 638–648. <https://doi.org/10.1002/mrc.4855>.
- Habib, M.A., Khoda, B., 2022. Rheological analysis of bio-ink for 3D bio-printing processes. J. Manuf. Process 76, 708–718. <https://doi.org/10.1016/j.jmapro.2022.02.048>.
- Handayati, Y., Widyanata, C., 2024. Effective food waste management model for the sustainable agricultural food Supply chain. Sci. Rep. 14 (1). <https://doi.org/10.1038/s41598-024-59482-w>.
- Herrada-Manchón, H., Fernández, M.A., Aguilar, E., 2023. Essential guide to hydrogel rheology in extrusion 3D printing: how to measure it and why it matters? Gels 9 (7), 517. <https://doi.org/10.3390/gels9070517>.
- Hooi Chuan Wong, G., Pant, A., Zhang, Y., Kai Chua, C., Hashimoto, M., Huei Leo, C., 2022. Tan, U.-X. 3D food printing—sustainability through food waste upcycling. Mater. Today Proc. 70, 627–630. <https://doi.org/10.1016/j.mtpr.2022.08.565>.
- Jergitsch, M., Allué-Mengual, Z., Perez, R.A., Mateos-Timoneda, M.A., 2023. A systematic approach to improve printability and cell viability of methylcellulose-

- based bioinks. *Int. J. Biol. Macromol.* 253, 127461. <https://doi.org/10.1016/j.ijbiomac.2023.127461>.
- Kim, H.W., Lee, J.H., Park, S.M., Lee, M.H., Lee, I.W., Doh, H.S., Park, H.J., 2018. Effect of hydrocolloids on rheological properties and printability of vegetable inks for 3D food printing. *J. Food Sci.* 83 (12), 2923–2932. <https://doi.org/10.1111/1750-3841.14391>.
- Lau, K.Q., Sabran, M.R., Shafie, S.R., 2021. Utilization of vegetable and fruit by-products as functional ingredient and food. *Front Nutr.* 8. <https://doi.org/10.3389/fnut.2021.661693>.
- Lee, C.P., Takahashi, M., Arai, S., Lee, C.-L.K., Hashimoto, M., 2021. 3D printing of okara ink: the effect of particle size on the printability. *ACS Food Sci. Technol.* 1 (11), 2053–2061. <https://doi.org/10.1021/acsfoodscitech.1c00236>.
- Li, H., Liu, S., Li, L., 2016. Rheological study on 3D printability of alginate hydrogel and effect of graphene oxide. *Int. J. Bioprint.* 2 (2), 54–66. <https://doi.org/10.18063/JB.2016.02.007>.
- Liu, Z., Bhandari, B., Zhang, M., 2020. Incorporation of probiotics (*Bifidobacterium Animalis Subsp. Lactis*) into 3D printed mashed potatoes: effects of variables on the viability. *Food Res. Int.* 128, 108795. <https://doi.org/10.1016/j.foodres.2019.108795>.
- Lynch, K.M., Steffen, E.J., Arendt, E.K., 2016. Brewers' Spent grain: a review with an emphasis on food and health. *J. Inst. Brew.* 122 (4), 553–568. <https://doi.org/10.1002/jib.363>.
- Malik, S., Kanhere, S.S., Jurdak, R., 2018. ProductChain: scalable blockchain framework to support provenance in supply chains. In: 2018 IEEE 17th International Symposium on Network Computing and Applications (NCA). IEEE, pp. 1–10. <https://doi.org/10.1109/NCA.2018.8548322>.
- Mao, J., Meng, Z., 2024. Fabrication and characterization of novel high internal phase bigels with high mechanical properties. *Ph. Invers. Pers. Edible 3D Food Print. Food Hydrocoll.* 153, 110019. <https://doi.org/10.1016/j.foodhyd.2024.110019>.
- Marcin, Mitrus, Leszek, Moscicki, 2009. Physical properties of thermoplastic starches. *Int. Agrophys.* 29.
- Mirazimi, F., Salido, J., Sepulcre, F., Gràcia, A., Pujola, M., 2022. Enriched puree potato with soy protein for dysphagia patients by using 3D printing. *Food Front.* 3 (4), 706–715. <https://doi.org/10.1002/fft2.149>.
- Molina-Montero, C., Matas, A., Igual, M., Martínez-Monzó, J., García-Segovia, P., 2023. Impact of apricot pulp concentration on cylindrical gel 3D printing. *Gels* 9 (3), 253. <https://doi.org/10.3390/gels9030253>.
- National Environment Agency (NEA) Singapore, 2021. Factsheet updates to Singapore's food waste management system (accessed on 15 June, 2025). <https://www.nea.gov.sg/docs/default-source/media-files/cos2021/cos2021-media-factsheet-mandatory-framework-for-food-waste-reporting.pdf>.
- National Environment Agency; Agri-Food & Veterinary Authority of Singapore, 2017. Food waste minimisation guidebook for Food Manufacturing Establishment (accessed on 15 June, 2025). <https://www.nea.gov.sg/docs/default-source/our-services/waste-management/food-waste-minimisation-guidebook-for-food-manufacturing-establishments.pdf>.
- Oyedele, A.B., Wu, J., 2023. Food-based uses of brewers spent grains: current applications and future possibilities. *Food Biosci.* 54, 102774. <https://doi.org/10.1016/j.fbio.2023.102774>.
- Pant, A., Lee, A.Y., Karyappa, R., Lee, C.P., An, J., Hashimoto, M., Tan, U.X., Wong, G., Chua, C.K., Zhang, Y., 2021. 3D Food printing of fresh vegetables using Food hydrocolloids for dysphagic patients. *Food Hydrocoll.* 114 (December 2020), 106546. <https://doi.org/10.1016/j.foodhyd.2020.106546>.
- Razavizadeh, S., Alencikiene, G., Salaseviciene, A., Vaiciulyte-Funk, L., Ertbjerg, P., Zubulionite, A., 2021. Impact of fermentation of Okara on physicochemical, technofunctional, and sensory properties of meat analogues. *Eur. Food Res. Technol.* 247 (9), 2379–2389. <https://doi.org/10.1007/s00217-021-03798-8>.
- Rodríguez-Herrera, V.V., Umeda, T., Kozu, H., Sasaki, T., Kobayashi, I., 2024. Printability of nixtamalized corn dough during screw-based three-dimensional food printing. *Foods* 13 (2), 293. <https://doi.org/10.3390/foods13020293>.
- Rysenaer, V.B.J., Ahmadzadeh, S., Van Bockstaele, F., Ubeyitogullari, A., 2023. An extrusion-based 3D food printing approach for generating alginate-pectin particles. *Curr. Res. Food Sci.* 6, 100404. <https://doi.org/10.1016/j.cfrs.2022.11.023>.
- Sagar, N.A., Pareek, S., Sharma, S., Yahia, E.M., Lobo, M.G., 2018. Fruit and vegetable waste: bioactive compounds, their extraction, and possible utilization. *Compr. Rev. Food Sci. Food Saf.* 17 (3), 512–531. <https://doi.org/10.1111/1541-4337.12330>.
- Sharma, R., Chandra Nath, P., Kumar Hazarika, T., Ojha, A., Kumar Nayak, P., Sridhar, K., 2024. Recent advances in 3D printing properties of natural food gels: application of innovative food additives. *Food Chem.* 432, 137196. <https://doi.org/10.1016/j.foodchem.2023.137196>.
- Shi, X., 2019. Printability of hydrogel composites using extrusion-based 3D printing and post-processing with calcium chloride. *Food Sci. Nutr.* 5 (2), 1–5. <https://doi.org/10.24966/FSN-1076/100051>.
- Sularz, O., Smoleń, S., Koronowicz, A., Kowalska, I., Leszczyńska, T., 2020. Chemical composition of lettuce (*Lactuca Sativa L.*) biofortified with iodine by KIO_3 , 5-iodo-, and 3,5-diiodosalicylic acid in a hydroponic cultivation. *Agronomy* 10 (7), 1022. <https://doi.org/10.3390/agronomy10071022>.
- Tejada-Ortigosa, V., Cuau-Urquiza, E., 2022. Towards the development of 3D-printed food: a rheological and mechanical approach. *Foods* 11 (9), 1191. <https://doi.org/10.3390/foods11091191>.
- Tomić, S.Ij., Radić, Babić, M., M., Vuković, J.S., Filipović, V.V., Nikodinovic-Runic, J., Vukomanović, M., 2023. Alginate-based hydrogels and scaffolds for biomedical applications. *Mar. Drugs* 21 (3), 177. <https://doi.org/10.3390/mdi21030177>.
- Voon, S.L., An, J., Wong, G., Zhang, Y., Chua, C.K., 2019. 3D Food printing: a categorised review of inks and their development. *Virtual Phys. Prototyp.* 14 (3), 203–218. <https://doi.org/10.1080/17452759.2019.1603508>.
- Wan, Y., Zhou, Q., Zhao, M., Hou, T., 2023. Byproducts of sesame oil extraction: composition, function, and comprehensive utilization. *Foods* 12 (12), 2383. <https://doi.org/10.3390/foods12122383>.
- Wang, Y., Zhang, X., Gao, Y., Yuan, F., Mao, L., 2023. Development of k-carrageenan hydrogels with mechanically stronger structures via a solvent-replacement method. *Food Innov. Adv.* 2 (4), 313–323. <https://doi.org/10.48130/FIA-2023-0031>.
- Waseem, M., Tahir, A.U., Majeed, Y., 2024. Printing the future of food: the physics perspective on 3D food printing. *Food Phys.* 1, 100003. <https://doi.org/10.1016/j.foodp.2023.100003>.
- Wypych, G., 2016. Physical properties of fillers and filled materials. *Handbook of Fillers*. Elsevier, pp. 303–371. <https://doi.org/10.1016/B978-1-895198-91-1.50007-5>.
- Xin, S., Deo, K.A., Dai, J., Krishna Rajeeva Pandian, N., Chimene, D., Moebius, R.M., Jain, A., Han, A., Gaharwar, A.K., Alge, D.L., 2021. Generalizing hydrogel microparticles into a new class of bioinks for extrusion bioprinting. Vol. 7. <http://www.science.org>.
- Xu, Y.Y., Howes, T., Adhikari, B., Bhandari, B., 2013. Effects of emulsification of fat on the surface tension of protein solutions and surface properties of the resultant spray-dried particles. *Dry. Technol.* 31 (16), 1939–1950. <https://doi.org/10.1080/07373937.2013.802331>.
- Yoha, K.S., Moses, J.A., 2023. 3D Printing approach to valorization of agri-food processing waste streams. *Foods* 12 (1), 212. <https://doi.org/10.3390/foods12010212>.
- Yu, H., Li, W., Feng, S., Loo, S.C.J., 2024. Impacts of industrial food wastes on nutritional value of mealworm (*tenebrio molitor*) and its gut microbiota community shift. *Biomater. Adv.* 165, 214022. <https://doi.org/10.1016/j.bioadv.2024.214022>.
- Zeko-Pivac, A., Tišma, M., Žnidarsić-Plazl, P., Kulisić, B., Sakellaris, G., Hao, J., Planinić, M., 2022. The potential of brewer's spent grain in the circular bioeconomy: state of the art and future perspectives. *Front Biogen Biotechnol.* 10 (June), 1–15. <https://doi.org/10.3389/fbioe.2022.870744>.
- Zhang, Y., Lee, A.Y., Pojchanun, K., Lee, C.P., Zhou, A., An, J., Hashimoto, M., Tan, U.-X., Leo, C.H., Wong, G., Chua, C.K., Pant, A., 2022. Systematic engineering approach for optimization of multi-component alternative protein-fortified 3D printing food ink. *Food Hydrocoll.* 131, 107803. <https://doi.org/10.1016/j.foodhyd.2022.107803>.
- Zhang, C., Wang, C.-S., Girard, M., Therriault, D., Heuzey, M.-C., 2024. 3D Printed protein/polysaccharide food simulant for dysphagia diet: impact of cellulose nanocrystals. *Food Hydrocoll.* 148, 109455. <https://doi.org/10.1016/j.foodhyd.2023.109455>.
- Zhong, R., Xu, X., Wang, L., 2017. Food supply chain management: systems, implementations, and future research. *Ind. Manag. Data Syst.* 117 (9), 2085–2114. <https://doi.org/10.1108/IMDS-09-2016-0391>.